Diagnosis of Ruptured Intracranial Dermoid Cyst: Value of MR over CT

Alison S. Smith[1,2]
Jane E. Benson[2,3]
Susan I. Blaser[4]
Akira Mizushima[1,5]
Robert W. Tarr[1]
Errol M. Bellon[2]

The CT and MR findings of seven patients with pathologically proved ruptured dermoid cysts were reviewed to analyze the MR characteristics and to see if MR evaluation had significant advantages over CT. In six cases, both CT and MR identified fatty material in the CSF spaces. Hemorrhage complicated preoperative diagnosis in one case. Patterns of extraaxial fat distribution were as follows: intraventricular fat/CSF levels (three patients), generalized subarachnoid spread (six patients), and localized subarachnoid spread with sulcal widening (one patient). There was no correlation between fat distribution and clinical symptoms. MR showed the vascular involvement better than CT did in five of seven cases, and showed extension of the cysts into the skull base in two cases. Signal intensity of the solid mass was low on T1-weighted MR images and inhomogeneously high on T2-weighted images, which correlated pathologically with the presence of crystal cholesterol, hair, sebaceous glands, and epithelial cells in all cases. On MR, brain parenchyma showed little edema or other reaction to the masses, which were typically large.

The value of MR over CT in the examination of ruptured dermoid cysts is the conspicuity of the extent of subarachnoid spread, involvement of the extraaxial structures, and evidence of vascular compromise, which can obviate angiography. MR had no advantage over CT in making the initial diagnosis of ruptured dermoid, but it would be the preferred preoperative study.

AJNR 12:175–180, January/February 1991; *AJR* 156; April 1991

In the past, it was thought that intracranial dermoid cyst rupture was uniformly fatal [1]. With CT, however, rupture of intracranial dermoid cysts has been well documented and shows a spectrum of brain involvement and symptomatology [2–7]. We retrospectively reviewed seven cases of ruptured dermoid cysts studied by MR and CT to determine the degree to which the two studies agreed or were complementary. These cases also add to the number of patients who have survived cyst rupture and surgery.

Materials and Methods

Seven cases of ruptured intracranial and dermoid cysts studied by MR were collected from four hospitals between September 1985 and February 1989. Patient data appear in Table 1. MR and CT examinations were reviewed retrospectively. MR evaluations were performed on a variety of scanners owing to referral patterns. Two were performed at 0.5 T, one at 1.0 T, three at 1.5 T, and one patient was scanned on a 0.15 T prototype unit. Intraarterial digital subtraction angiography was performed in five cases, three of which were available for review. All patients had pathologic confirmation of the dermoid cyst by craniotomy. Follow-up varied from 6 months to 3 years.

Results

In all cases, pathologic study showed the presence of an epithelial cyst wall and a mass containing epithelial cells, cholesterol crystals, hair, and sebaceous glands.

Received September 7, 1989; revision requested November 13, 1989; revision received July 16, 1990; accepted July 30, 1990.

[1] Department of Radiology, University Hospitals of Cleveland, 2074 Abington Rd., Cleveland, OH 44106. Address reprint requests to A. S. Smith.

[2] Department of Radiology, MetroHealth Medical Center, Cleveland, OH 44109.

[3] Department of Radiology, Johns Hopkins Hospital, Baltimore, MD 21205.

[4] Department of Special Studies and Neuroradiology, Hospital for Sick Children, Toronto, Ontario, Canada.

[5] Present address: Kyushu University, Kukuoka, Japan.

0195-6108/91/1201-0175

Sweat glands were not specifically reported. No comments were made on the ratio of cholesterol or keratin. In five cases, the cysts were found in a very similar location; that is, in the parasellar region (cases 1–5). The masses in the other two cases were in the left frontal lobe extending into the lateral ventricle and in the sylvian fissure (cases 6 and 7, respectively).

The bright intensity of the fat on the short TR/short TE MR images subjectively made the fat more conspicuous in cases 1 through 6. Three patterns of fat distribution were apparent. In cases 1 through 3, material of high signal intensity relative to brain on short TR/short TE images resulted in a fluid/fluid level with CSF within the ventricles (Fig. 1). This finding correlated with the fat density seen on CT examination.

The fat was seen in extraventricular subarachnoid spaces in cases 1 through 6. The distribution was non–gravity dependent. Foci of fat above and below a narrowed aqueduct of Sylvius and fourth ventricle involvement were additional findings in case 2 (Fig. 2). The third pattern of fat distribution followed and widened the sulci in case 3 (Fig. 3). On long TR/long TE images, this material was iso- to hypointense relative to brain.

On short TR/short TE images, the solid component of the parasellar or intraparenchymal masses was low in intensity relative to brain with areas of isointense soft tissue and less prominent areas of hyperintensity. Long TR/long TE images showed the core or solid component of the mass to be inhomogeneously bright (Fig. 4). The latter correlated with surgical reports of the solid masses found to contain cholesterol crystals, epithelial lining, and hair and/or sebaceous glands. Case 7 was complicated by subacute and remote hemorrhage. The core mass in the sylvian fissure was of low intensity relative to the large bloody cyst on short TR/short TE images (Fig. 5). At surgery, the mass was green, solid, and contained dense cholesterol crystals, blood, and a focus of ossification. On the surgical report, the lesion was considered ruptured due to the presence of satellite lesions extending from the intraparenchymal mass into and widening the sylvian fissure.

Involvement of the orbital apex was clearly evident by MR,

TABLE 1: Clinical Symptoms and Imaging Studies in Seven Patients with Ruptured Intracranial Dermoid Cysts

Case No.	Age (years)	Sex	Presentation	CT	MR	Angiography	Surgery	Follow-up
1	23	F	5 yr history of headache, new visual symptoms	01/30/88	02/02/88	02/24/88	03/03/88	Required shunting at 3 weeks
2	24	F	Dermoid diagnosed at age 9, new visual symptoms	1983, 1986 04/21/87	1983 11/09/87	1983	1973	Another recurrence in 1989
3	43	M	New seizure, headache for 2 days, 1 month of blurred vision	06/07/88	06/09/88	06/10/88	06/14/88	Doing well at 1 yr
4	35	M	Acute hemiparesis, 8 yr history of anisocoria	10/22/87	11/11/87	11/30/87	12/01/87	Doing well at 6 months
5	49	M	New seizures, benign brain tumor removed 10 yr earlier	04/16/88	05/03/88	N.A.	04/16/88	Post-op confusion, slight improvement at 6 months
6	45	F	Progressive seizures and aphasia, over 2 yr	09/27/85	05/22/85	(01/20/86)	01/21/86	Doing well at 1 yr
7	80	F	Acute confusion and right hemiparesis	02/08/89	02/08/89	(06/88)	02/13/89	Did well until died of pulmonary embolism 2/27/89

Note.—Parentheses indicate study unavailable for review.

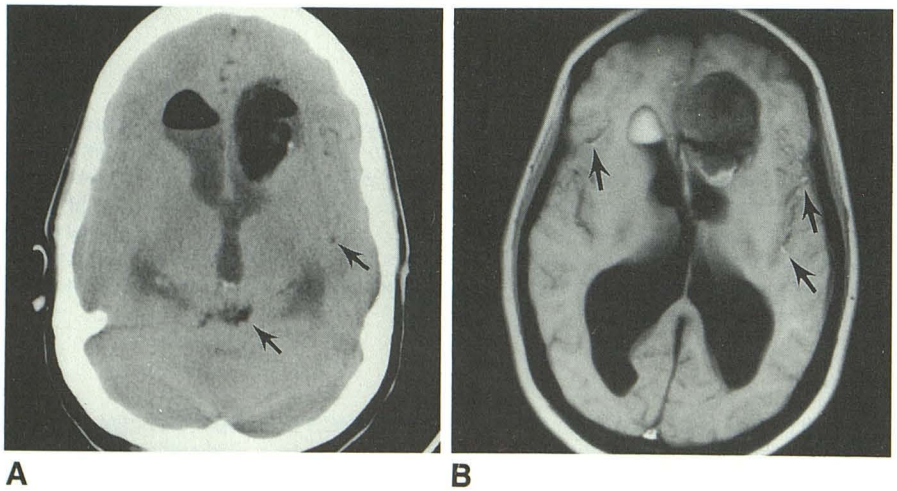

A B

Fig. 1.—Case 1: 23-year-old woman with 5-year history of intermittent headaches associated with leg weakness. A mass of heterogeneous soft tissue and fat, which extended from the parasagittal region, intrudes into frontal horn of left lateral ventricle. Fat/CSF level is seen within right lateral ventricle. Fat globules can also be seen scattered within other subarachnoid spaces (*arrows*).

***A*, Unenhanced CT scan.**

***B*, T1-weighted (400/14) MR image shows better delineation of fat from extraventricular CSF compared with CT scan.**

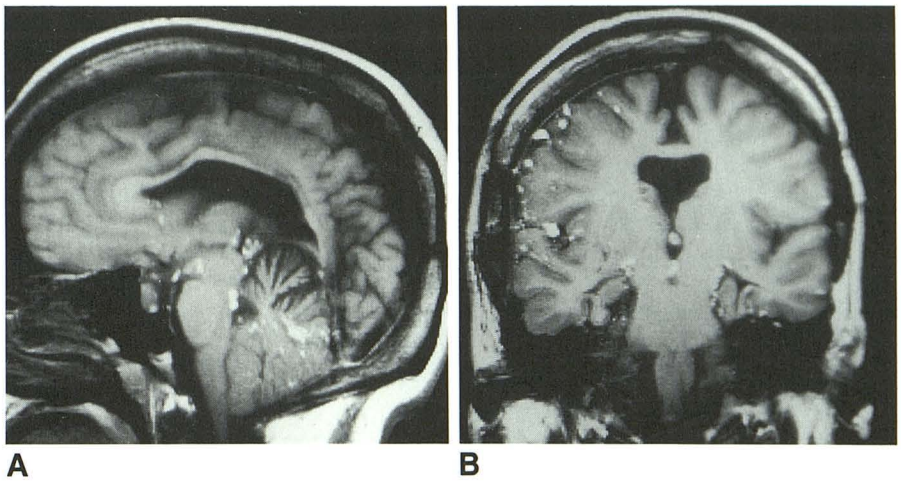

Fig. 2.—Case 2: 24-year-old woman who had a ventriculostomy shunt placed at 7 weeks of age for aqueductal stenosis, and debulking of a left middle fossa dermoid at ages 9 and 19. The patient also had multiple congenital defects including an absence of the septum pellucidum and aqueductal stenosis.

A and *B*, Sagittal (*A*) and coronal (*B*) T1-weighted (500/20) MR images show fat signal within third and fourth ventricles and extensive subarachnoid seeding.

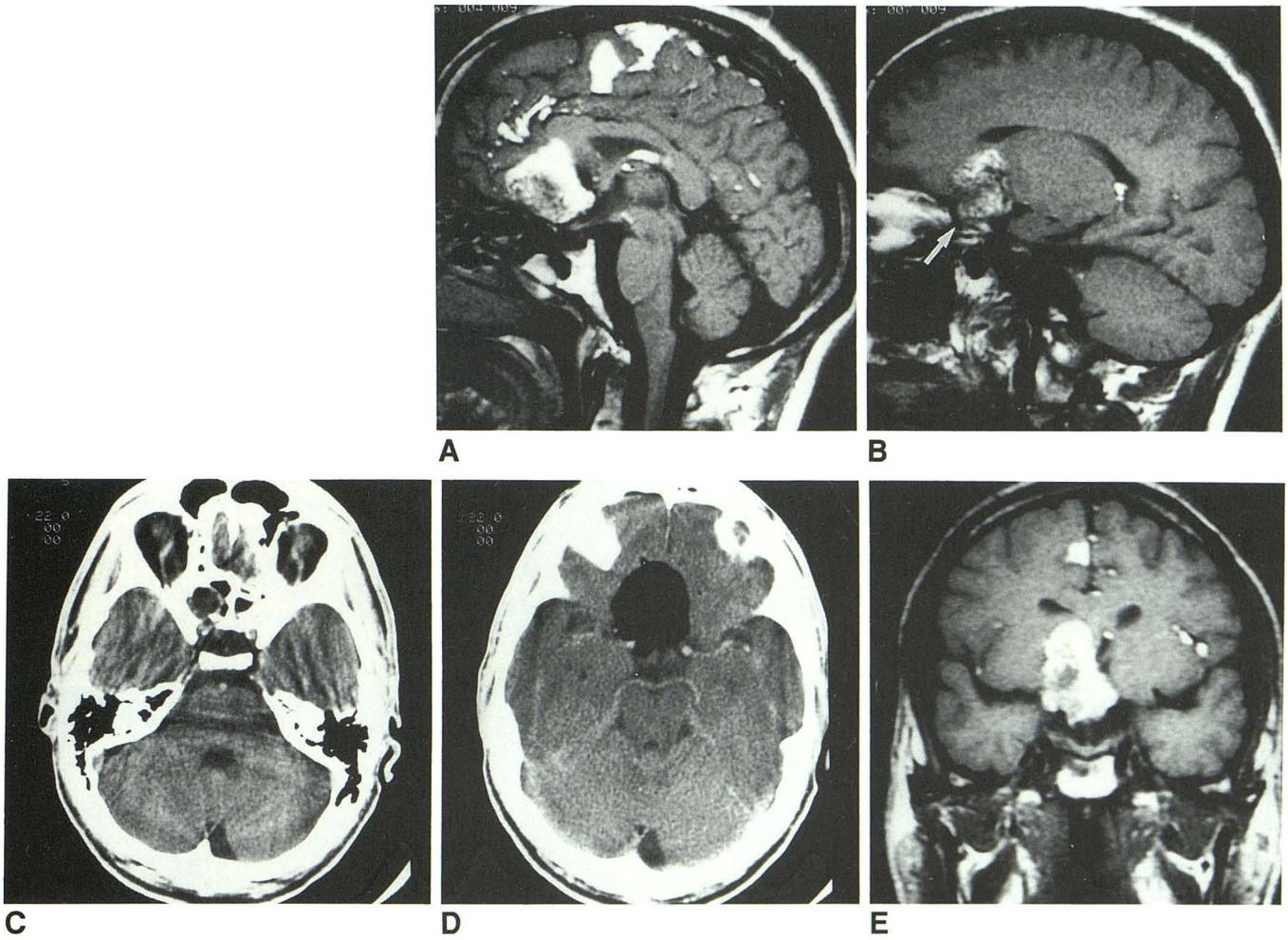

Fig. 3.—Case 3: 43-year-old man who presented with headache and 1 month of blurred vision.

A, T1-weighted (500/20) MR image shows suprasellar mass of heterogeneous signal intensity. Material of increased signal intensity widens the sulci at the interhemispheric fissure.

B, T1-weighted (500/20) MR image shows impingement on orbital apex by mass (*arrow*).

C, CT scan shows mass at orbital apex but impingement on orbit must be surmised.

D, CT scan at region of chiasm indicates some encroachment.

E, Coronal T1-weighted (600/20) MR image shows chiasm nearly engulfed by the mass.

while only suspected by CT in cases 2 and 3. Involvement of the optic chiasm in case 3 was also dramatically demonstrated. Both of these patients had visual symptoms. Angiographic correlation was available in three cases. Displacement and encasement of the right internal carotid artery and displacement of the basilar and right posterior cerebral arteries were predicted by MR in case 4 and confirmed by angiography (Fig. 4).

MR accurately predicted displacement without encasement of the anterior cerebral arteries in cases 1 and 3. Cases 2 and 7 clearly showed flow void within the displaced middle cerebral arteries, but angiographic correlation was not available. Case 5 did not have angiographic or CT/MR suggestion of major vessel displacement. Patient 6 was imaged on a 0.15-T prototype unit and the study was inadequate for evaluation of vessels. There was no evidence of edema in parenchyma surrounding the dermoid cysts by CT or MR examination. Ventricular enlargement was present in four patients (cases 1, 4, 5, 7), three with interstitial edema (cases 4, 5, 7). Small-rim calcifications seen by CT in cases 3, 4, and

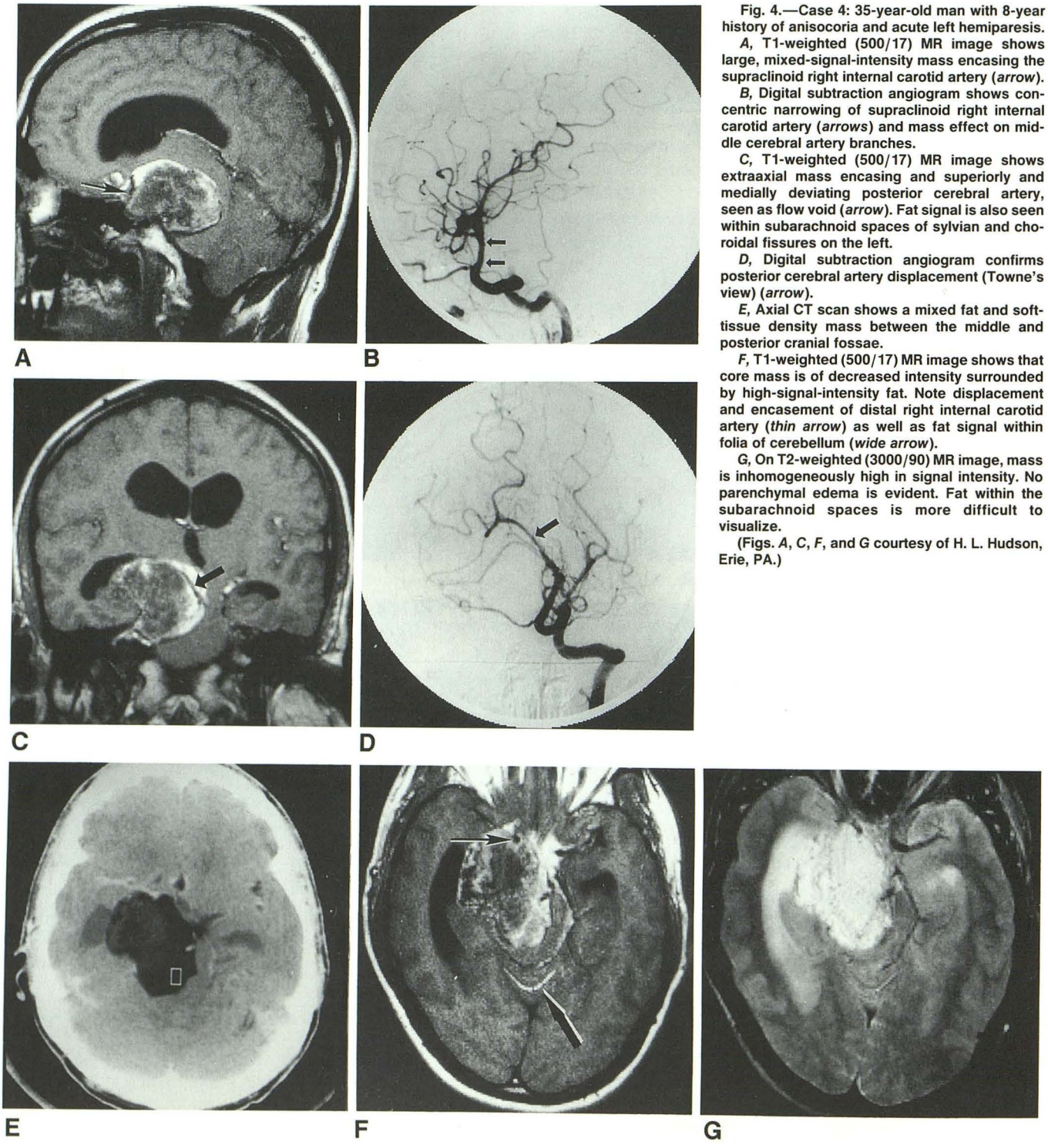

Fig. 4.—Case 4: 35-year-old man with 8-year history of anisocoria and acute left hemiparesis.

***A,* T1-weighted (500/17) MR image shows large, mixed-signal-intensity mass encasing the supraclinoid right internal carotid artery (*arrow*).**

***B,* Digital subtraction angiogram shows concentric narrowing of supraclinoid right internal carotid artery (*arrows*) and mass effect on middle cerebral artery branches.**

***C,* T1-weighted (500/17) MR image shows extraaxial mass encasing and superiorly and medially deviating posterior cerebral artery, seen as flow void (*arrow*). Fat signal is also seen within subarachnoid spaces of sylvian and choroidal fissures on the left.**

***D,* Digital subtraction angiogram confirms posterior cerebral artery displacement (Towne's view) (*arrow*).**

***E,* Axial CT scan shows a mixed fat and soft-tissue density mass between the middle and posterior cranial fossae.**

***F,* T1-weighted (500/17) MR image shows that core mass is of decreased intensity surrounded by high-signal-intensity fat. Note displacement and encasement of distal right internal carotid artery (*thin arrow*) as well as fat signal within folia of cerebellum (*wide arrow*).**

***G,* On T2-weighted (3000/90) MR image, mass is inhomogeneously high in signal intensity. No parenchymal edema is evident. Fat within the subarachnoid spaces is more difficult to visualize.**

(Figs. *A*, *C*, *F*, and *G* courtesy of H. L. Hudson, Erie, PA.)

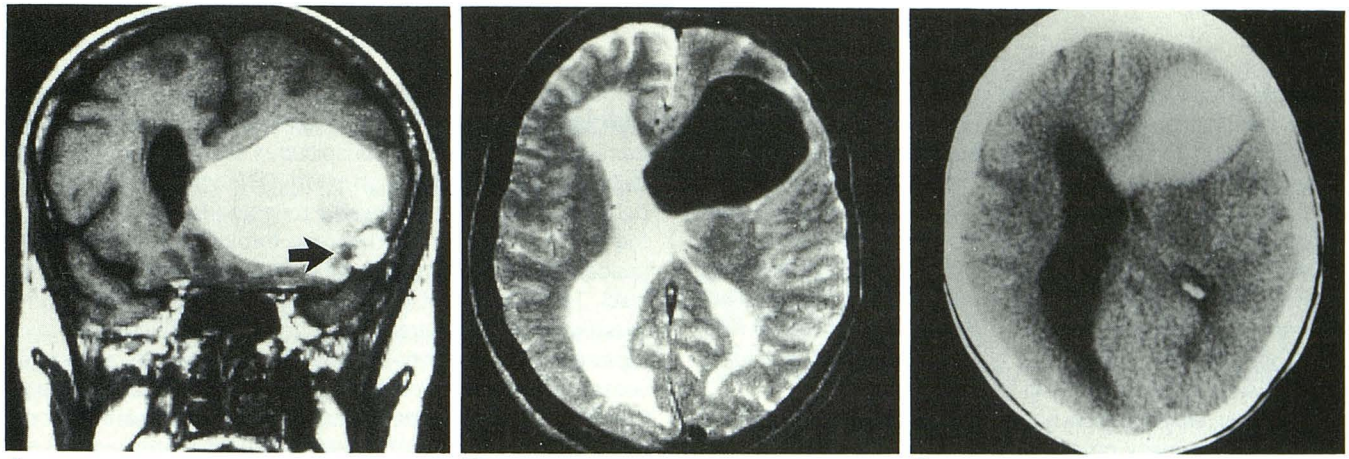

Fig. 5.—Case 7: 80-year-old woman with acute confusion, right hemiparesis, and frontal headaches of several months duration.
***A*, T1-weighted (500/20) MR image shows large hyperintense mass within left frontal parenchyma ruptured into sylvian fissure. The hypointense focus (*arrow*) was a solid mass of cholesterol crystals.**
***B*, T2-weighted (2400/120) MR image shows that marked hypointensity of cyst correlates with the presence of acute blood.**
***C*, CT scan confirms the presence of blood and paucity of edema.**

5 were not definable by MR. On follow-up two of seven patients required ventricular shunts for enlarging ventricular size [1, 5].

Discussion

Dermoid cysts are within the category of epithelial cysts. Their location in the midline or posterior fossa and their presentation in the first two to three decades of life helps to differentiate dermoids from epidermoids. Epidermoids tend to present in the fifth decade and are less often in the midline, frequently at the cerebellopontine angle [8, 9]. Like epidermoid cysts, intracranial dermoid cysts are thought to originate from ectodermal inclusions from defects of closure at approximately 3 to 5 weeks gestation [10]. Histologically, the dermoid cyst has a lining of stratified squamous epithelial cells, a feature shared with epidermoid cysts. Unlike epidermoid cysts, however, dermoid cysts can contain additional elements of hair or sebaceous or sweat glands [8, 11]. These additional dermal elements are of ectodermal origin [12]. The presence of all epidermal layers in dermoid cysts leads to the theory that they originated from the inclusion of a slightly more primitive, pluripotential cell than that which gives rise to epidermoid cysts [10]. The elements of the dermoid cyst can vary in relative proportions. In general, there is a thick, viscous, greenish-brown fluid composed of lipid metabolites and liquid cholesterol from decomposed epithelial cells. Cholesterol crystals result in more lumpy masses. Hair can be present as a few strands or a matted clump [11]. Calcifications of dental enamel, another ectodermal derivative, are present less often [13].

The liquid products of lipid metabolism and cell breakdown and resulting increased hydrogen density could explain the increased signal intensity seen on short TR/short TE images within the subarachnoid and intraventricular spaces. The liquid nature of the fatty acids and liquid portion of the cholesterol may affect the protons available for use in MR signal. Protons bound to cholesterol crystals, hair, and intact cells of the solid tumor mass are less available to yield an MR signal; thus, this part of the mass is hypo-to isointense relative to brain. The inhomogeneous signal on long TR/long TE images from the more solid core of the mass reflects the mixture of intact and partially degenerated materials of the hair, glandular elements, and more solid cholesterol.

The CT characteristics of ruptured dermoid cysts were first described by Fawcitt and Isherwood in 1976 [2] and are typified by fat/CSF levels within the ventricles and/or fat densities in subarachnoid spaces [4, 5]. An extraaxial or combined extra- and intraaxial soft-tissue mass is present. Although, this is not the first report of MR findings of ruptured dermoid cyst, to the best of our knowledge, the cases presented here are the first MR demonstration of the imaging characteristics and utility of MR in diagnosing this disease.

This series demonstrates three patterns of distribution for the spilled contents of intracranial dermoid cysts. The classic CT appearance of fat/fluid levels in the ventricles was present in less than half the cases (three of seven). The first six cases also displayed extraventricular subarachnoid spread, six of which were diffuse. The images show that the non–gravity-dependent fat is not merely trapped between sulci, implying that it is adherent. The first MR report of ruptured intracranial dermoid by Hahn et al. [14] displayed the curious finding of sulci widened by fat deposits on short TR/short TE images. This third pattern of localized spread in sulci, as seen in case 3 in our series, may represent ruptured contents contained by pia or inflammatory tissue. Indeed, this may have been the appearance of case 7 (Fig. 5) prior to hemorrhage, since thick inflammatory reaction encasing the extension of the mass into the sylvian fissure was present at surgery. The possibility that the pattern of fat distribution may relate to the chronicity of the rupture and the patient's symptoms was considered. It was tempting to surmise that fat/fluid levels may correlate with more recent cyst rupture and the localized fat with sulcal widening due to a more chronic, indolent leak. This hypothesis was not borne out by the clinical data in this series of patients.

Aside from the ease of multiplanar imaging, MR has additional advantages over CT in imaging dermoid cysts as demonstrated by these cases. The extent of the mass and the relation to the skull base was more easily evaluated by MR because of the lack of bone artifacts. Five of these large

dermoid cysts extended from the parasellar region of the skull base, invaginating deeply into brain parenchyma. No evidence of connection to the skull could be seen on MR or CT to suggest a definable dermal sinus, which is often associated with posterior fossa dermoids [10, 15]. Possible connections to the skull (i.e., at the areas of otic and optic closure) may be small, but Currarino and Rutledge [16] suggest they may be more common than previously thought. Indeed, the patient in case 4 was known to have an intraorbital dermoid on the side opposite the intracranial lesion as well as a midline parietal skull defect, indicating faults in closure.

Generally, epidermoids have been reported as areas of hypo- to isointensity on short TR/short TE images [17]. Six of seven of our cases of dermoids displayed high signal on short TR/short TE images. However, in a minority of cases the T1 signal is not a reliable criterion for the MR differentiation of dermoids from epidermoids. Epidermoids have been reported to have areas of high signal on short TR/short TE sequences [18, 19]. The opposite situation has been reported in which two proved dermoids and two lipomas have yielded low signal on T1- and T2-weighted images at 0.15 T [20]. We have seen two cases of recurrent dermoid having only an isointense mass. Since the complications of dermoids and epidermoids are similar, the lack of specificity in these occasional cases with varying MR characteristics is probably of less clinical significance than the size and location of the mass. The lack of MR visualization of calcification seen by CT is of no clinical significance.

We were impressed by the large size of the lesions relative to the lack of edema in these patients at the time of presentation. The slow rate of growth and their tendency to extend through subarachnoid spaces along the base of the brain is reflected in the relative paucity of symptoms in relation to tumor size [9]. The most frequent symptoms are headache, seizure, dementia, meningitis, and transient ischemic attacks associated with arterial spasm. The latter has been associated temporally with rupture of the cysts [2] and was probably implicated as the cause of hemiparesis in cases 2 and 5 of this series. In general, however, symptoms may not be related to the time of rupture [5] and may be a response to the cholesterol rather than lipid content [4]. Five of our cases showed compression or displacement of intracranial vessels. In this retrospective review, four of the cases had correlative angiography. However, the MR, especially if paired with MR angiography, should obviate conventional angiography for evaluation of arterial anatomy on a prospective basis.

Earlier studies reported that the rupture of an intracranial dermoid with consequent ventriculitis and meningitis was fatal [1]. The cases in this series add to the body of patients surviving rupture and subsequent removal of intracranial dermoid cysts [4, 6, 7]. However, chronic arachnoiditis does appear to be a frequent sequela. The rate of occurrence of bleeding into a dermoid cyst or association with rupture is unknown.

In summary, MR had no advantage over CT for the initial diagnosis of ruptured intracranial dermoid cyst. The MR characteristics were that of a relatively large mass, which was usually parasellar. This mass contained a solid portion that was of decreased signal on short TR/short TE images and of mixed intensity on long TR/long TE images, corresponding to pathologic findings of cholesterol crystals, epithelial lining, and glandular structures. The spread of the liquid contents of the dermoid cyst was more conspicuous on MR than CT owing to bright signal intensity on short TR/short TE images. The patterns of the fat signal were reflected in fat/fluid levels in the ventricles, generalized spread through the subarachnoid spaces, and a pattern of more limited spread within widened sulci. The duration of patient symptoms could not be correlated with the appearance of the fat distribution and cyst rupture. The capability of MR to evaluate the associated vessel displacement, either by flow void or MR angiography, paired with better visualization of the lesions relative to the base of the skull owing to lack of bone interference and multiplanar imaging capability, make MR the preferred preoperative imaging method. The cases in this series also add to the number of patients who have survived rupture of intracranial epithelial cysts.

REFERENCES

1. Manlapaz JS. Ruptured intracranial dermoid: report of a case and survey of previously reported cases. *Am J Surg* **1960**;100:723–730
2. Fawcitt RA, Isherwood I. Radiodiagnosis of intracranial pearly tumors with particular reference to the value of computed tomography. *Neuroradiology* **1976**;11:235–242
3. Ford K, Drayer B, Osborne D, Dubois P. Case report: Transient cerebral ischemia as a manifestation of ruptured intracranial dermoid cyst. *J Comput Assist Tomogr* **1981**;5:895–897
4. Amendola MA, Garfinkle WB, Ostrum BJ, Katz MR, Katz RI. Preoperative diagnosis of a ruptured intracranial dermoid cyst by computerized tomography. Case report. *J Neurosurg* **1978**;48:1035–1037
5. Laster DW, Moody DM, Ball MR. Epidermoid tumors with intraventricular and subarachnoid fat: report of 2 cases. *AJR* **1977**;128:504–507
6. Hamer J. Diagnosis by computerized tomography of intradural dermoid with spontaneous rupture of the cyst. *Acta Neurochir* (Wien) **1980**;51: 219–226
7. Healy JF, Brahme FJ, Rosenkrantz H. Dermoid cysts and their complications as manifested by computed cranial tomography. *Comput Tomogr* **1980**;4:111–115
8. Rubinstein LJ. *Atlas of tumor pathology,* second series, fasicle 6. Bethesda, MD: Armed Forces Institute of Pathology, **1972**:228–292
9. Fleming R, Botterell EH. Cranial dermoid and epidermoid tumors. *Surg Gynecol Obstet* **1959**;109:403–411
10. Schijman E, Monges J, Cragnaz R. Congenital dermal sinuses, dermoid and epidermoid cysts of the posterior fossa. *Childs Nerv Syst* **1986**;2: 83–89
11. Martin J, Davis L. Intracranial dermoid and epidermoid tumors. *Arch Neurol Psychol* **1943**;49:56–70
12. Smith AS. Myth of the mesoderm: ectodermal origin of dermoids. *AJNR* **1989**;8:449
13. Arey LB. *Developmental anatomy.* Philadelphia: Saunders, **1982**: 89, 230–235
14. Hahn FJ, Ong E, McComb RD, et. al. MR imaging of ruptured intracranial dermoid. *J Comput Assist Tomogr* **1986**;10:888–892
15. Tytus JS, Pennybacker J. Pearly tumors in relation to the central nervous system. *J Neurol Neurosurg Psychiatry* **1959**;19:241–259
16. Currarino G, Rutledge JC. Temporoparietal dermoid cysts with intracranial extension. *AJNR* **1988**;9:385–387
17. Tampieri D, Melanson D, Ethier R. MR imaging of epidermoid cysts. *AJNR* **1989**;10:351–356
18. Mackay IM, Bydder GN, Young IR. MR imaging of central nervous system tumors that do not display increase in T1 or T2. *J Comput Assist Tomogr* **1985**;9:1055–1061
19. Lee BCP, Kneeland JB, Deck MDF, Cahill PT. Posterior fossa lesions: magnetic resonance imaging. *Radiology* **1984**;153:137–143
20. Latack JT, Kartush JM, Kenink JL, et. al. Epidermoidomas of the cerebellopontine angle and temporal bone: CT and MR aspects. *Radiology* **1985**; 157:361–366